

Article

Nitrate Reduction through Al-Fe Alloy Catalyst: Effects of Activation Pre-Treatment Method and Alloy Type

Xin Ma ¹, Lei Zheng ^{1,2,*}, Zifu Li ^{1,2}, Lingling Zhang ^{1,2}, Shikun Cheng ^{1,2}  and Xuemei Wang ^{1,2}

¹ School of Energy and Environmental Engineering, University of Science and Technology Beijing, Beijing 100083, China

² Beijing Key Laboratory of Resource-Oriented Treatment of Industrial Pollutants, University of Science and Technology Beijing, Beijing 100083, China

* Correspondence: zhengl@ustb.edu.cn; Tel./Fax: +86-10-8237-6638

Abstract: This study explored the nitrate reduction by Al-Fe alloy. The nitrate conversions of fresh, 30-day and 90-day alloys were 78.1%, 42.8% and 9.5%, respectively. Water activation promoted the reducing ability of the alloy (98% nitrate removal), which was higher than that of copper deposited alloy (66%) and H₂-reducing/acid/alkali/Cl⁻ activated alloy (no enhancement). The effects of pre-treatments on the surface O fraction changes confirmed the activation results. With increased Fe:Al mass ratio in the alloy, nitrate conversion initially decreased and then increased again, verifying the proposed electron-donor activity of Al or Fe in alloys. Al-Fe₃₀ had the highest NO₃⁻ conversion and Al₁₃Fe₄ content, so Al-Fe₃₀ was selected. Significant differences in conversion were observed in alloy usages of 5–10 and 15–30 g/L. High reduction performance (nitrate below the detection limit and 19.1% N₂ selectivity) was achieved under the optimal conditions: 15 g/L Al-Fe₃₀, 150 min reaction and without pH adjustment. The rate constants of nitrate removal, nitrogen generation and ammonia generation were $k_1 = 1.43 \times 10^{-2}$, $k_2 = 3.41 \times 10^{-2}$ and $k_3 = 10.58 \times 10^{-2} \text{ min}^{-1}$, respectively. The value of $(k_2 + k_3)/k_1$ was 10, indicating that the conversion of nitrate into nitrite was the rate-determining step. The repetition reaction was performed, and the rate constant decreased as the reaction step was repeated.

Keywords: nitrate reduction; Al-Fe alloy type; activation pre-treatment; intermetallic compound; Al₁₃Fe₄



Citation: Ma, X.; Zheng, L.; Li, Z.; Zhang, L.; Cheng, S.; Wang, X. Nitrate Reduction through Al-Fe Alloy Catalyst: Effects of Activation Pre-Treatment Method and Alloy Type. *Water* **2023**, *15*, 3122. <https://doi.org/10.3390/w15173122>

Academic Editor: Chi-Wang Li

Received: 18 July 2023

Revised: 9 August 2023

Accepted: 14 August 2023

Published: 31 August 2023



Copyright: © 2023 by the authors. Licensee MDPI, Basel, Switzerland. This article is an open access article distributed under the terms and conditions of the Creative Commons Attribution (CC BY) license (<https://creativecommons.org/licenses/by/4.0/>).

1. Introduction

Nitrate is one of the most ubiquitous pollutants, and an excessive nitrate concentration in the environment can lead to severe pollution problems, such as river eutrophication, water quality deterioration and potential hazards to human health [1], indicating the need for its proper disposal prior to being discharged to the environment.

Compared with other treatment processes, chemical reduction has been widely applied due to its better nitrate removal performance, lower reaction time and easier management. Previous studies have used zero-valent iron (Fe⁰) as the main reductant in removing contaminants in water [2]. Fe⁰ is a reactive metal that is considered an effective reductant for NO₃⁻ removal due to its non-toxicity, abundance, low cost and easy maintenance in the reduction process. In this system, nitrate removal performance mainly depends on lower pH [3]. In particular, ammonia was the dominant by-product of the reduction process that required another system to deal with it [4]. Thus, nitrate removal was incorporated with catalytic components, such as Pd, Pt and Au, to improve the N₂ selection [5].

Many studies have investigated the use of Fe combined with precious metal catalysts for nitrate removal from water. These previous studies posited that nitrate reduction was hindered by the limitations of low pH requirements and the high cost of precious metal catalysts, suggesting that a more promising system that can reduce nitrate should

be developed [6]. To address this gap, this study proposed the nitrate removal through an Al-Fe alloy containing intermetallic $\text{Al}_{13}\text{Fe}_4$ to satisfy the abovementioned requirements.

The adsorption properties of intermetallic compounds are different to elements and substitutional solid solutions, which is the key to the selectivity in heterogeneous catalysis [7]. $\text{Al}_{13}\text{Fe}_4$ was identified as a low-cost replacement for Pd-based hydrogenation catalysts, which are assigned to the combination site isolation and alteration of the electronic structure through chemical bonding [7]. The 1,3-butadiene hydrogenation on the $\text{Al}_{13}\text{Fe}_4$ surface was investigated and confirmed to be as active as Pd [8].

$\text{Al}_{13}\text{Fe}_4$ can be induced as a low-cost alternative to Pd in nitration reduction. $\text{Al}_{13}\text{Fe}_4$ can be formed on the iron-poor side of the Al-Fe phase diagram. This study investigated the nitration removal by the Al-Fe alloy. According to previous studies [9], Al-Fe alloys contain Al or Fe together with intermetallic compounds, including $\text{Al}_{13}\text{Fe}_4$. The nitrate reduction by Al-Fe alloy could be expected through the following mechanism: Al or Fe may serve as electron donors in Al-Fe alloys while $\text{Al}_{13}\text{Fe}_4$ was used as a low-cost alternative to Pd for nitrate reduction.

To date, few published reports have described the Al-Fe alloy-based nitration reduction. Jie Xu et al. [10,11] investigated aluminum–iron alloy particles for nitrate removal and revealed that Al-Fe alloys efficiently reduced nitrate in water in a pH range of 2–12. Limited studies have conducted a systematic evaluation of Al-Fe-alloy-based nitrate reduction that focused on the effects of alloy type (previous studies tested three typical alloys: AlFe10, AlFe20 and AlFe58, which are commonly design for material utility). When aged during storage, the thickness of the aluminum or iron oxide layer on the alloy particles surface will increase, suggesting that the inactive effects of these compounds on nitrate reduction cannot be ignored. Xu jie [10] has found that the deionized water pre-treatment was better than HCl and KBH_4 for alloy activation. The study will analyze the effects of different pre-treatment method, including H_2 -reducing pre-treatment, copper deposition pre-treatment, acid/alkali/ Cl^- activation pre-treatment and water activation pre-treatment on the nitrate reduction.

2. Material and Methods

2.1. Materials

All chemicals, such as sodium nitrate (NaNO_3), cupric chloride dehydrate ($\text{CuCl}_2 \cdot 2\text{H}_2\text{O}$), hydrochloric acid (HCl) and sodium hydroxide (NaOH), were of analytical grade. These reagents were purchased from Shanghai Chemical Reagents Company (Shanghai, China). Zero iron powder and zero aluminum powder (<0.07 nm, >98%) were obtained from Sinopharm Chemical Reagent Beijing Co., Ltd. (Beijing, China) Distilled water was used in all experiments (Ultrapure water system standard type, OKP-S040, Shanghai Laike Industrial Development Co., Ltd. (Shanghai, China)).

2.2. Methods

2.2.1. Synthesis of Al-Fe Alloys

Desired compositions of the Al and Fe powders were added to a MgO crucible with mass ratios of 8:2 (denoted as Al-Fe20), 7:3 (denoted as Al-Fe30), 6:4 (denoted as Al-Fe40), 5:5 (denoted as Al-Fe50), 4:6 (denoted as Al-Fe60) and 3:7 (denoted as Al-Fe70). Abbreviations indicated the original synthesis mass ratio of Al to Fe powders. All alloys used in this study were pre-reacted by heating the powders in an induction furnace to 1250 °C under inert Ar atmosphere in ceramic Al_2O_3 crucibles. This temperature is higher than the specific liquid's temperature but well below the melting temperature of the high-melting-point elements. The Al-Fe ingot was crushed by P1000-MUODE Alloy crusher into particles, and the 0.5–1.5 mm particles were used in this study. To analyze Al or Fe together with intermetallic compounds in Al-Fe alloys, mineralogical analysis was conducted on the prepared alloys by X-ray powder diffraction (XRD, Rigaku D/MAX-RB, Akishima, Tokyo, Japan).

2.2.2. Experimental Design

H₂-reducing pre-treatment: The Al-Fe alloy was heated to 400 °C under H₂/N₂ flow (20 vol% H₂, 50 mL/min) and maintained for 3 h. The alloy was cooled to room temperature under H₂/N₂ flow, and the reduced alloy was purged by helium gas (50 mL/min) for 10 min. The H₂-reduced alloy was stored in a dry box.

Copper deposition pre-treatment: Copper precursors were dissolved in distilled water at a concentration of 1000 mg/L. The desired amount of copper precursors was added to the alloy particles while stirring, and the mass ratio of the copper to the alloy was 4.00% (*w/w*). Then, the mixture was washed twice with water, filtered using a laboratory 0.45 µm membrane and then dried via a vacuum freeze-drying technique.

Acid/alkali/Cl⁻ activation pre-treatment: Alloy particles were added to centrifuge tubes containing HCl solution (0.25 mol/L; solution-to-solid-mass ratio, 10), NaOH solution (0.25 mol/L; solution-to-solid-mass ratio, 10) and NaCl solution (0.25 mol/L; solution-to-solid-mass ratio, 10). The mixture was stirred with an overturning rotator at 80 r/min and 20 °C for 3 h. The particles were washed with distilled water until pH value was stable (determined by pH meter), filtered using a laboratory 0.45 µm membrane and then dried via a vacuum freeze-drying technique.

Water activation pre-treatment: Alloy particles were added to centrifuge tubes containing distilled water at a water-to-solid-mass ratio of 10. The centrifuge tubes were sealed with screw caps, and the mixture was stirred at 80 r/min and 50 ± 1 °C for 3 h. The mixture was filtered using a laboratory 0.45 µm membrane and then dried via a vacuum freeze-drying technique. According to preliminary study, the induction time of Al-Fe alloy at 30 °C, 40 °C, 50 °C and 60 °C were 48.5 h, 21.8 h, 2.7 h and 1.6 h, respectively. In this study, 50 °C and 3 h were chosen for water activation parameters.

Nitrate reduction experiment: First, an artificial solution (40 mg/L NaNO₃) was prepared for the batch experiments. The pre-treatment analysis in this study revealed that, compared with other pre-treatment methods, the water activation pre-treatment substantially promoted the reducing ability. All of the alloys used in other parts of this study were pretreated by water activation method. The reducing performances of the alloys under different operational conditions (alloy type, reaction time and amount of alloys) were investigated. All tests were performed in 150 mL necked flasks. Exactly 100 mL of nitrate solution (NaNO₃) was added to each flask containing the desired type and amount of alloy. All flasks were placed in an electronic oscillator and stirred at 250 r/min and room temperature (the room temperature was about 20–25 °C during this study). The nitrate reaction container was conducted without temperature adjustment. As the reaction of Al with water is exothermal, the reaction of Al with water is self-heating. In this case, the water temperature would increase from room temperature to about 30–35 °C. Three to six samples of each time were tested, averaging the experimental values obtained (the average results and errors bars are all shown in the results section).

To test the reusability of the alloys, nitrate reduction experiments were conducted in four consecutive cycles. At the end of each reduction experiment, the nitrate concentration in the solution was measured. Then, the initial nitrate concentration was adjusted to 40 mg/L by adding nitrate stock solution.

2.2.3. Methods of Analysis

Samples were collected periodically from the flasks to determine the nitrate, nitrite and ammonium concentrations. The determination procedures for the following nitrogen forms were referenced from the literature: nitrite-nitrogen (NO₂⁻-N): spectrophotometric method (GB 7493-87); nitrate-nitrogen (NO₃⁻-N): ultraviolet spectrophotometry (HJ/T 346-2007); and ammonium (NH₄⁺-N): Nessler's Reagent Spectrophotometry (HJ 535-2009).

The nitrate conversion efficiency and the catalytic selectivity to N₂ were calculated as follows:

$$\text{Nitrate conversion efficiency (\%)} = \frac{C_0 - C_t}{C_0} \times 100\% \quad (1)$$

$$N_2 \text{ selectivity (\%)} = \frac{2C_{N_2}}{C_0 - C_t} \times 100\% \quad (2)$$

where C_0 is the initial nitrate concentration in the solution (mg/L), C_t is the nitrate concentration (mg/L) at time t (min), and C_{N_2} is the amount of N_2 produced (mg/L). N_2 content was calculated by a quantity balance under the assumption that the produced NO_x was negligible.

3. Results and Discussion

3.1. Effects of Pre-treatment Methods on Alloy Activation Performance

Nitrate conversion through Al-Fe alloys suffers from aging during storage, as shown in Figure 1a, in which Al-Fe20 was used as a representative Al-Fe alloy. The nitrate conversion efficiencies of fresh, 30-day and 90-day alloys were 78.1%, 42.8% and 9.5%, respectively, demonstrating a progressive decrease with increasing storage time.

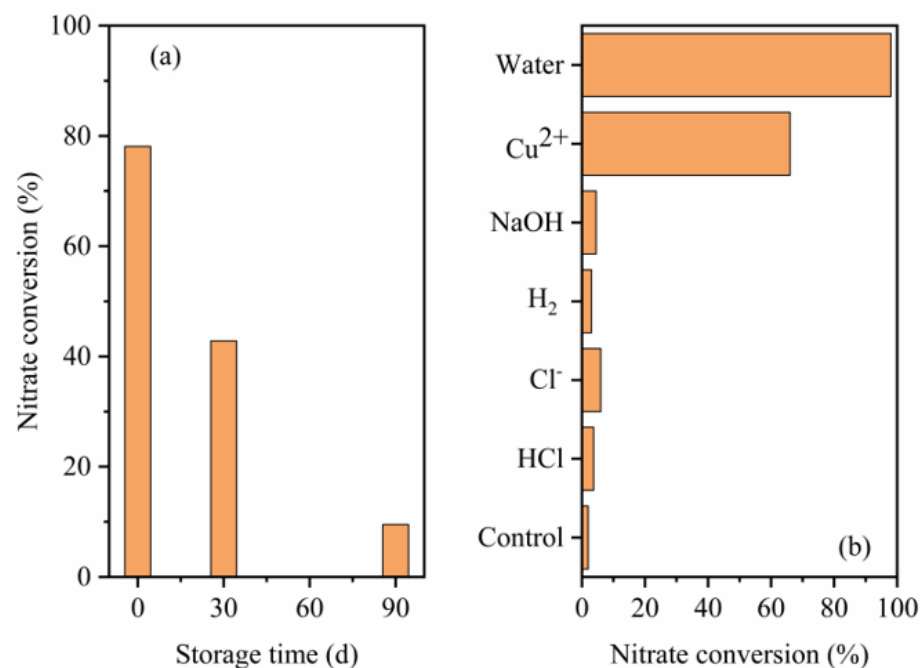


Figure 1. Effects of alloy (a) storage time and (b) activation pre-treatment method on the nitrate conversion.

Al or Fe were used to react with water for hydrogen generation. It is known that aluminum under usual conditions is inactive to reactions of oxidation by water. A dense oxide film can form on an alloy surface during storage, which against Al or Fe to generate hydrogen at room temperature condition. The nitrate reduction efficiency using these alloys will decrease as shown in the study (Figure 1a).

When making Al or Fe react with water, there is an induction time, which is the activation time of the native oxide film, after which H_2 generation occurs [12]. To shorten the induction time, different activation methods have been investigated, based on the disruption of passive oxide layers on metal particles. H_2 -reducing pre-treatment was proven to be an effective removing method for passive iron oxide layers on Fe particles, and so, it was conducted in this paper. On the other hand, several measures for passive aluminum oxide removal on Al particles have been developed, e.g., alkaline or acid solution pre-treatment, ball milling, soluble inorganic salt and graphite activation, and high temperature surface modification, etc. Considering the activation method should be cost effective and easy for application, the method adopted for study in this paper was weak acid or alkali treatment and mild temperature water activation.

Figure 1b illustrates the nitrate conversion by the 90-day alloy and the counterpart alloys under different pre-treatment methods. Water activation and copper deposition

pre-treatment substantially promoted nitrate conversion, and the ultimate nitrate reduction efficiency of the water-activated-alloy-based system (98%) was higher than that of the copper deposited alloy-based system (66%). When other activation pre-treatments were introduced, including H₂-reducing pre-treatment and acid/alkali/Cl⁻ activation pre-treatment, the nitrate reduction efficiencies remained low and nearly the same as that of the control.

The H₂-reducing pre-treatment of zero valent iron at 400 °C enhanced the removal of nitrate at a pH of 6.5–7.5 [13]. The nitrate reduction by the Al-Fe alloy after H₂-reducing pre-treatment was the same as that of the control. This phenomenon can be due to the stable behavior of the alumina oxide under H₂-reducing pre-treatment because Al is a stronger reductant than H₂ and Fe (standard potentials of Al³⁺ ⇌ Al (s), Fe²⁺ ⇌ Fe (s) and Fe³⁺ ⇌ Fe²⁺ were −1.676, −0.44 and 0.771, respectively), which can inhibit the passive layer reduction of the alumina oxide by H₂.

Acid or alkali pre-treatment has been proven to recover the reducing ability of zero aluminum powder [14]. However, the lack of effect of the acid/alkali on the Al-Fe alloy activation in this study can be explained by two factors: (1) the corrosion activity energy of aluminum is lower than that of the Al alloy, such that the alloy was more stable than pure metal under normal conditions; and (2) the acid/alkali concentration used in this study was too small. Strong acid or alkali was unsuitable because of the additional costs, and acid or alkali liquid not only induced pollution but also damaged the reactor's instrument.

A previous study [15] showed that Cl⁻ can induce a passivity breakdown and pitting erosion to metallic materials, such as Al and Fe. McCafferty [16] developed a pitting erosion model. In this model, the Cl⁻ on the oxide surface is adsorbed. Then, the Cl⁻ ions are transported through the oxide film, followed by the dissolution of the Al at the metal–oxide interface. For the Al-Fe alloy, constituent particles such as Al₁₃Fe₄ in alloys induce the heterogeneity of the oxide surface, leading to the local adsorption of Cl⁻ and reducing the Cl⁻ corrosion of the alloy. A previous study obtained a similar result that the pitting erosion on the alloy surface by Cl⁻ can be passivated by intermetallic compounds, such as Al₁₃Fe₄ [17].

In this study, copper deposition pre-treatment stimulated the Al-Fe alloy to reduce nitrate. This finding was consistent with a previous study in which copper salt was added to promote nitrate reduction kinetics by nanoscale zero valent iron [18]. A similar mechanism can be concluded that copper ions imposed electrochemical reactions to stimulate iron or aluminum corrosion and then boost nitrate reduction removal efficiency.

To optimize the water activation parameters, the effect of water temperature on the induction time was conducted. The results showed that the induction time of Al-Fe alloy at 30 °C, 40 °C, 50 °C and 60 °C were 48.5 h, 21.8 h, 2.7 h and 1.6 h, respectively. To save heating energy, 50 °C and 3 h were chosen for water activation parameters in this study. The water activated alloy shows high reduction efficiency when used for nitrate removal as shown in Figure 1b, indicating the induction process of alloy has been finished after it was activated at 50 °C for 3 h.

The water activation mechanism for alloy could be deduced from previous studies about Al powder reaction with water. Owing to the passive oxide film on the surface, the pure Al powder could react with water and generate hydrogen, but it has an induction time, for example many days at 25 °C [19]. The induction time decreases with increasing the reaction temperature, which is nearly 6, 3 and 1 h for the temperatures of 30 °C, 40 °C and 50 °C, respectively [20].

When Al particle is put into water for H₂ generation, there is a series of reactions [20]:
① A hydration reaction between the passive oxide on Al particle surface and water. One Al-O-Al linkage is broken to form two AlOOH (thermodynamically more stable than Al₂O₃ at room temperature) for each water molecule consumed.
② When the hydrated front came in contact with the inside metal, Al reacted with water and generated hydrogen.
③ H₂ molecules accumulated to form small H₂ bubbles at the Al–Al₂O₃ interface. When the gas pressure in the H₂ bubbles exceeded the threshold that the hydrated oxide film can

sustain, the film on the Al-Fe alloy particle surfaces breaks, and the hydrogen generation from Al continues. The hydrolysis process can modify the oxide lattice and replacing O_2^- ions with more mobile species. Secondary ion mass spectrometry (SIMS) has been used in conjunction with isotopic labeling to determine the passive film hydration on aluminum, suggesting that water molecules are the mobile species in the films (rather than H^+ , O^{2-} or Al^{3+}) [21]. The higher water temperature could promote water transport during hydration steps and speed up the accumulation of H_2 molecules in H_2 bubbles to reach the critical gas pressure, resulting in the decrease in the induction time.

As the alloy used in the study is particles with a 0.5–1 mm size, the induction time may be longer than Al powders as the larger Al particles have a larger total tolerable extension of their oxide films and the H_2 bubbles at their Al: Al_2O_3 interfaces. On the other hand, KwangSup Eom [22] designed Al-Fe alloys for fast on-board hydrogen production and found that the electrochemically noble Al_3Fe (the same phase to $Al_{13}Fe_4$) in alloy precipitates along grain boundaries, which cause faster hydrogen generation from the hydrolysis of Al by combined action of galvanic and intergranular corrosion. $Al_{13}Fe_4$ in Al-Fe alloy synthesized in the study may also shorten the induction time through the similar mechanism.

After the passive film hydration finished, the metal Al could react with water and the product is $Al(OH)_3$. As the reaction proceeds, the products will cover the surface. Whether this new formed $Al(OH)_3$ film could stop the reaction between metal and water should be considered. When the Al powder used for H_2 generation, the reaction continues until the metal Al is consumed completely. As for the particle used in this paper (0.5–1 mm), it was found that the new formed $Al(OH)_3$ on the surface also did not terminate the reaction in these results (see the repetitive reduction performance discussed later). Xu jie [10] found that the deionized water pre-treatment was better than HCl and KBH_4 for alloy activation, which was consistent with the results that water activation is efficient for Al-Fe alloy reduction reaction.

Table 1 presents the EDX surface analysis results of different alloys, and the O fraction changes on the surface of the different alloys were consistent with Figure 1. The O fraction significantly increased relative to the storage time increment, indicating that an air-formed passive oxide film was formed on the alloy surface. When the aged alloy was treated with water activation pre-treatment or copper deposition, the oxide film was reduced, as indicated by the lower O fraction. The alloys displayed limited O fraction reductions after other pre-treatment reactions. This finding was consistent with the low nitrate conversion enhancement by these pre-treatments.

Table 1. EDX surface analysis results of different alloys.

Alloys	Elemental Fraction (wt%)		
	O	Al	Fe
Fresh alloy	3.1	68.1	28.8
30-day alloy	9.7	61.7	28.6
90-day alloy	17.3	57.7	25
Water activated alloy	5.2	67.4	27.4
Copper deposited alloy	9.8	60.4	29.8
H_2 -reduced alloy	16.9	54.1	29
Acid activated alloy	16.6	58.9	24.5
Alkali activated alloy	16.7	54.8	28.5
Cl^- activated alloy	15.8	57.6	26.6

3.2. Effects of Alloy Type and Amount on Nitrate Reduction

The nitrate reduction efficiency was controlled by alloy type with different Fe:Al mass ratios, as shown in Figure 2. With increased Fe:Al mass ratio, the nitrate conversion initially decreased and subsequently increased again after a certain value of this parameter. According to previous research [23], several structurally complex intermetallic compounds could be

formed during alloy synthesis. The characteristics of the alloys are presented in Figure 3. The major crystalline phases in the alloys were Al, Fe and different intermetallic compounds (in this study, six intermetallic compounds were found: Al_6Fe , $\text{Al}_{13}\text{Fe}_4$, Al_5Fe_2 , Al_2Fe , AlFe and AlFe_3), as shown in Figure 3. The peak of Al was observed in the four Al-rich alloys, and the peak intensities followed the order of $\text{Al-Fe20} > \text{Al-Fe30} > \text{Al-Fe40} > \text{Al-Fe50}$, demonstrating a progressive decrease with increasing Fe:Al mass ratio in the alloy. On the other hand, the Fe peak appeared in the three Fe-rich alloys, and the peak increased in the order of $\text{Al-Fe50} < \text{Al-Fe60} < \text{Al-Fe70}$. For the intermetallic compounds, Al-rich intermetallic compounds tended to form in the alloys with higher Al:Fe mass ratios and vice versa (See Figure 3): Al_6Fe and $\text{Al}_{13}\text{Fe}_4$ were found in Al-Fe20 ; $\text{Al}_{13}\text{Fe}_4$ was found in Al-Fe30 and Al-Fe40 , Al_5Fe_2 and $\text{Al}_{13}\text{Fe}_4$ were found in Al-Fe50 ; Al_2Fe and AlFe were found in Al-Fe60 ; and AlFe_3 was found in Al-Fe70 .

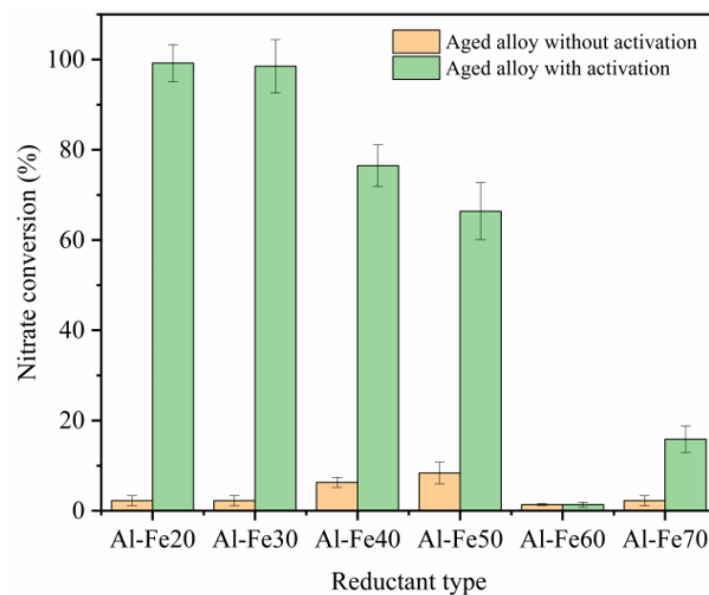


Figure 2. Variations of nitration conversion with respect to Al-Fe alloy types (90-day alloys with and without water activation) at a constant original nitration of 40 mgN/L and 4 h reaction time.

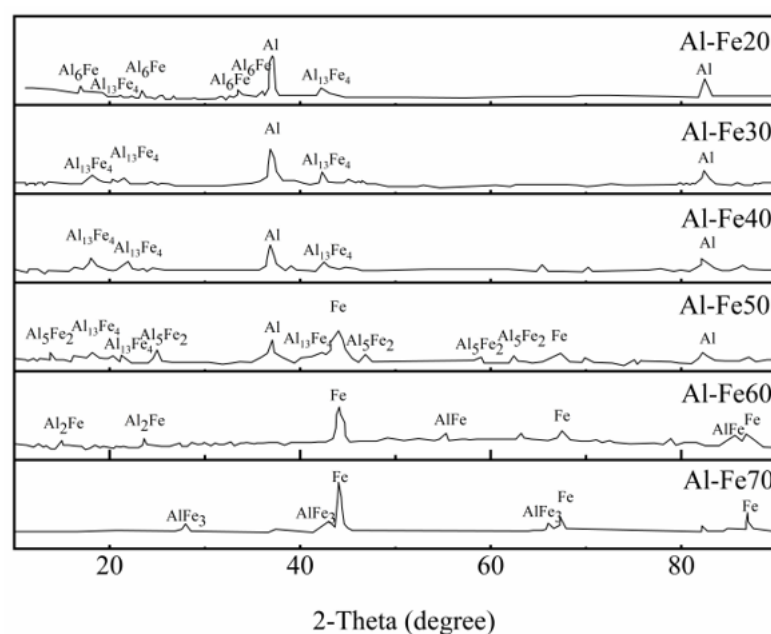


Figure 3. XRD patterns of different Al-Fe alloys.

The nitrate reduction efficiency behavior using different alloy types (Figure 2) could be explained by the XRD results and the proposed nitrate mechanism. According to the XRD results, Al-Fe alloys contain Al or Fe together with $\text{Al}_{13}\text{Fe}_4$. On the other hand, $\text{Al}_{13}\text{Fe}_4$ was confirmed as a low-cost alternative to Pd in heterogeneous hydrogenation [7], indicating that the nitrate reduction by these Al-Fe alloys can be deduced from previous studies using zero Fe and Pd. The nitrate removal mechanism using zero Fe and Pd has confirmed that [24] zero-valent iron acted as electron donors and reacted with H_2O to produce H_2 . Then, hydrogen attached onto the metal active sites, thereby reducing nitrate into nitrite. According to previous study, the intermediate product nitrite further was reduced by Pd-Hads to form ammonium and nitrogen gas [25]. The possible nitrate reduction mechanism by Al-Fe alloy was: Al or Fe may also serve as electron donors in Al-Fe alloys. Different intermetallic compounds in aluminum iron alloys are effective catalytic substances, so XRD analysis was used to analyze different alloy samples. On the one hand, it ensures the success of the alloy preparation process. On the other hand, it determines the types of intermetallic compounds in different alloys. As shown in Figures 2 and 3, the Al content in the four Al-rich alloys followed the order of $\text{Al-Fe}_{20} > \text{Al-Fe}_{30} > \text{Al-Fe}_{40} > \text{Al-Fe}_{50}$, and the nitrate conversion decreased following the same order. As for Al-Fe_{60} , no Al peak was found in the XRD results, thus the nitrate conversion efficiency was the lowest. Compared with the Al-Fe_{60} , the Fe content increased in Al-Fe_{70} , resulting in higher reduction conversion in Al-Fe_{70} system. The alloys containing more Al or Fe showed higher nitrate conversions (U-shaped pattern in Figure 2), confirming the hypothesized electron donor activity of Al or Fe in Al-Fe alloys. The XRD results of Al-Fe_{30} before and after nitrate reduction were shown in Figure S2. Compared with the original Al-Fe_{30} , the peak intensity of Al decreased and the $\text{Al}(\text{OH})_3$ peak appeared in the alloy after nitrate reduction, which confirmed the electron donor activity of Al. Al has a stronger reducibility than Fe. As such, Al-rich alloys reached higher nitrate conversions, as shown in Figure 2.

As mentioned, $\text{Al}_{13}\text{Fe}_4$ can serve as a Pd catalyst. A higher $\text{Al}_{13}\text{Fe}_4$ may favor the selective decomposition of aqueous nitrate into nitrogen. Among the alloy types examined, Al-Fe_{20} and Al-Fe_{30} showed nearly the same activity for NO_3^- conversion. A higher $\text{Al}_{13}\text{Fe}_4$ content in Al-Fe_{30} may result in a higher N_2 selective production. The details on the N_2 selective performance will be presented later. On the basis of these results, Al-Fe_{30} was selected for further analyses.

The amount of alloy greatly affected the nitrate conversion performance, as shown in Figure 4. The nitrate conversion curves for 15–30 g/L alloy systems showed a rapid increase in the first 2 h, followed by a leveling off. The ultimate conversion efficiency of the reaction conducted by 15–30 g/L alloy was almost 100%. When 5–10 g/L alloy was used, the curve increased with time and did not become stable. Significant differences in the final conversion efficiencies were observed between 5–10 g/L and 15–30 g/L. The reaction period was prolonged as the amount became lower than 15 g/L, and 15 g/L was adopted in the next part.

The nitrate reduction was conducted in near-neutral pH solution ($\text{pH} = 7.2$) to simulate the application environment and the evolution of pH during the reduction process as shown in Figure S1. In the initial reduction, the pH value increased rapidly and then followed by a plateau phase. The final pH value of the solution after Al-Fe alloy based nitrate reduction was 9.44, which is alkali and needs further treatment before discharging.

Al-Fe alloy is a low-cost material similar with Fe^0 and was introduced as an alternative to Fe^0 for nitrate reduction in this study. In the Fe^0 system, nitrate removal performance mainly depends on lower pH and nitrate reduction produces ammonium ions under laboratory conditions that required another system to deal with it [26]. Compared with the traditional reduction of nitrate by Fe^0 , the proposed Al-Fe-alloy-based process can transform higher parts of nitrate into N_2 (19.1%) even at the neutral pH of the solution.

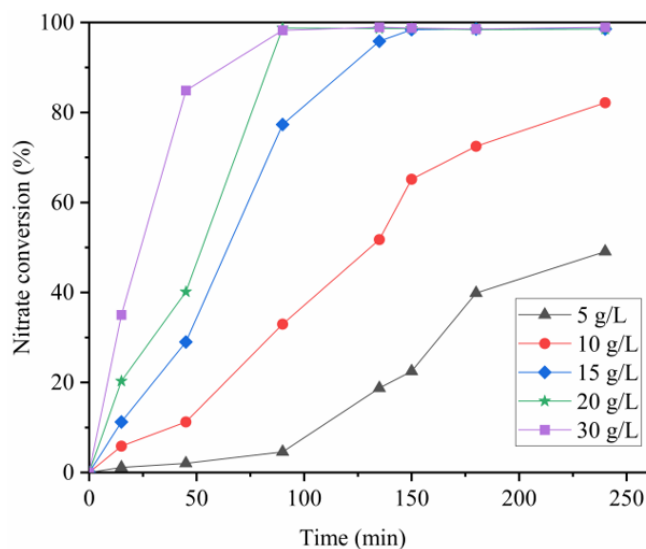


Figure 4. Variations of nitrate concentration with respect to Al-Fe30 amount.

The preliminary result in this study showed that N₂ selective production remained low (19.1%) and requires further improvement. This may be attributed to the fraction of Al₁₃Fe₄ in the alloy synthesized in this study that is still limited (XRD results). Another synthesis method is now under development in the author’s lab, which aims at the improvement of intermetallic component content in the Al-Fe alloy and the possible N₂ selective production improvement.

3.3. Kinetic and Repetitive Reduction Performance of Al-Fe30 Based Nitrate Removal

In order to distinguish whether nitrate is removed through degradation or adsorption, this study analyzed the product distribution, as shown in Figure 5. Reaction time affected the reduction performance of the Al-Fe alloy. The nitrate concentration steadily decreased with increased contact time, falling below the limit of detection within 150 min. Both the ammonium and N₂ conversions increased over time, reaching approximately 32.23 and 7.65 mg/L, respectively. The ultimate N₂ selectivity was approximately 19.1% after 150 min of reaction. These results demonstrated that a sufficient contact time between the alloy and the solution is necessary for nitrate removal, and 150 min was selected as the optimal time.

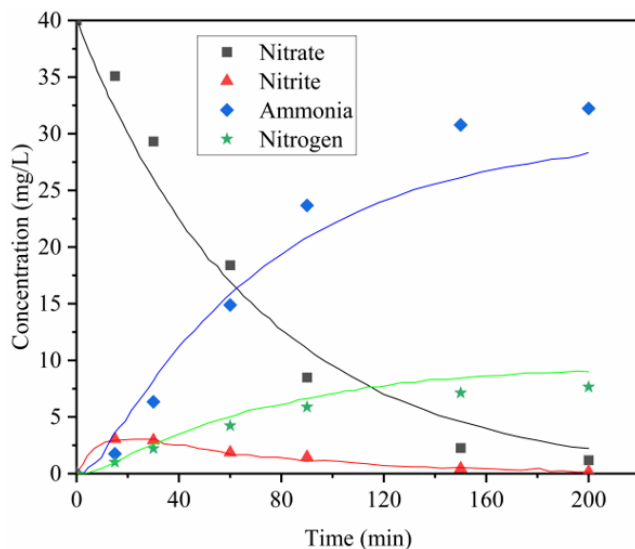
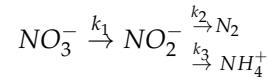


Figure 5. Variation of nitrogen-containing compounds with respect to time and fitted curves. Reduction parameters: 15 g/L Al-Fe30; original nitrate, 40 mg/L.

As shown in Figure 5, the concentration of NO_2^- increased at the initial stage of the reaction and then decreased after 60 min of the reaction. These results clearly indicated that nitrite is an intermediate to the final products, such as NH_4^+ and N_2 .

Therefore, nitrate reduction can be explained by reaction pathways as follows [27]:



An application of excel gauge solution based on the mode of linear programming was used to optimize reaction orders, and the results were shown in Table S1. The optimized order was 0.958799, and the correlation coefficient at this order was 0.988772. The reaction order was round up to 1 in this study. The disappearance of nitrate was described by a pseudo first-order kinetic model in which the rate is proportional to the dissolved substrate concentration in this study.

Thus the k_1 – k_3 are first-order rate constants, and the kinetic analysis was considered as in the following equation:

$$\frac{dC_{\text{NO}_3^-}}{dt} = -k_1 C_{\text{NO}_3^-} \quad (3)$$

$$\frac{dC_{\text{N}_2}}{dt} = -k_2 C_{\text{NO}_2^-} \quad (4)$$

$$\frac{dC_{\text{NH}_4^+}}{dt} = -k_3 C_{\text{NO}_2^-} \quad (5)$$

$$\frac{dC_{\text{NO}_2^-}}{dt} = k_1 C_{\text{NO}_3^-} - k_2 C_{\text{NO}_2^-} - k_3 C_{\text{NO}_2^-} \quad (6)$$

where C (mgN/L) is the concentration; k (min^{-1}) is the rate constant; and t (min) is the cumulative reaction time.

The k_1 value of the nitrate conversion rate constant was first estimated using the nitrate concentration developed with time. By adopting the obtained k_1 value, the other model parameters in Equation (6) can be estimated using the nitrite concentration. The result of the nonlinear regression analysis from this step is the sum of k_2 and k_3 . Given that the value of k_2/k_3 is identical to the slope of the C_{N_2} – $C_{\text{NH}_4^+}$ curve, the values of k_2 and k_3 can also be fitted. The fitting processes were conducted as described. The fitting results are presented in Table 2, and the curves are plotted in Figures 5 and 6.

Table 2. Calculated kinetic results.

	Parameter					
	k_1 (min^{-1})	$k_2 + k_3$ (min^{-1})	$(k_2 + k_3)/k_1$	Slope of C_{N_2} – $C_{\text{NH}_4^+}$	k_2 (min^{-1})	k_3 (min^{-1})
Value	0.01433	0.14001	10	0.24366	0.03411	0.10589
Adj. R-Square	0.97832	0.9893	-	0.98525	-	-

Table 2 indicates that the values of k_1 , k_2 and k_3 are 1.43×10^{-2} , 3.41×10^{-2} and $10.58 \times 10^{-2} \text{ min}^{-1}$, respectively. $(k_2 + k_3)/k_1$ is 10, as obtained by the curve fitting on the nitrate and nitrite concentrations. As shown, nitrite reduction was much faster than nitrate reduction. To convert nitrate into nitrogen and ammonia, the conversion of nitrate into nitrite is the rate-determining step.

To estimate the repetition of nitrate reduction by Al-Fe30, an experiment was conducted in which nitrate was repeatedly spiked into the reactor every 400 min. The pseudo-first-order kinetic model (proven zboce) was used to fit the experimental data, and the experimental results are summarized in Figure 7, which shows that the reduction was repeated four times until the reduction level was significantly reduced. Furthermore, the

rate of the nitrate reaction gradually decreased as the reaction step was repeated. The reaction rate constants from the first to the last steps were 1.43, 0.51, 0.26 and $0.11 \times 10^{-2} \text{min}^{-1}$. This phenomenon was possibly due to two reasons: (1) the oxidized Al or Fe formed an insoluble oxide layer on the surface that thickened as the reduction proceeded, hindering the penetration of nitrate ions; and (2) the available Al acting as electron donors were significantly diminished under repetitive reactions. These proposed reasons were confirmed with the XRD results as shown in Figure S2. The peak of Al oxide was found in the alloys after nitrate reduction, and the peak intensity increased as the reaction step was repeated. On the other hand, the peak intensity of Al was decreased as the reaction step was repeated, indicating the Al consuming as electron donor.

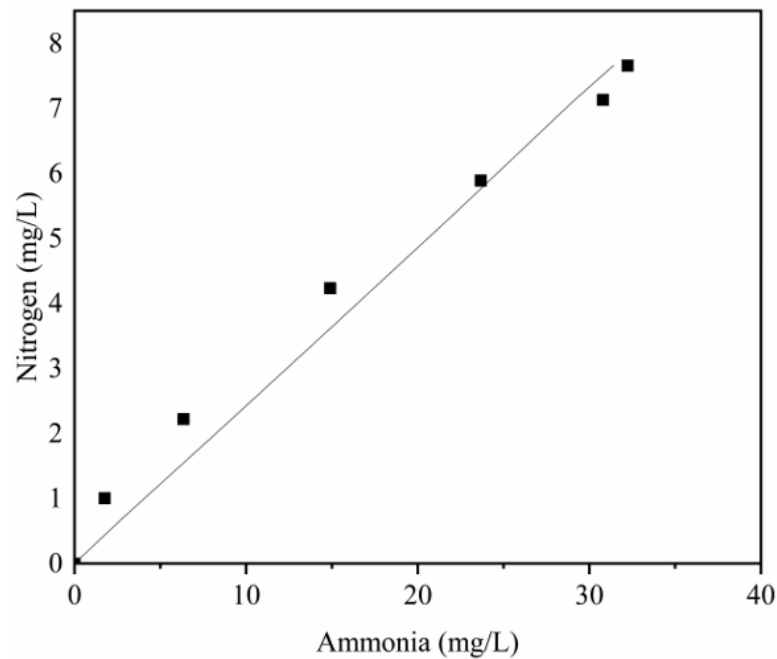


Figure 6. Linear fitting of nitrogen concentration with ammonia concentration for different times.

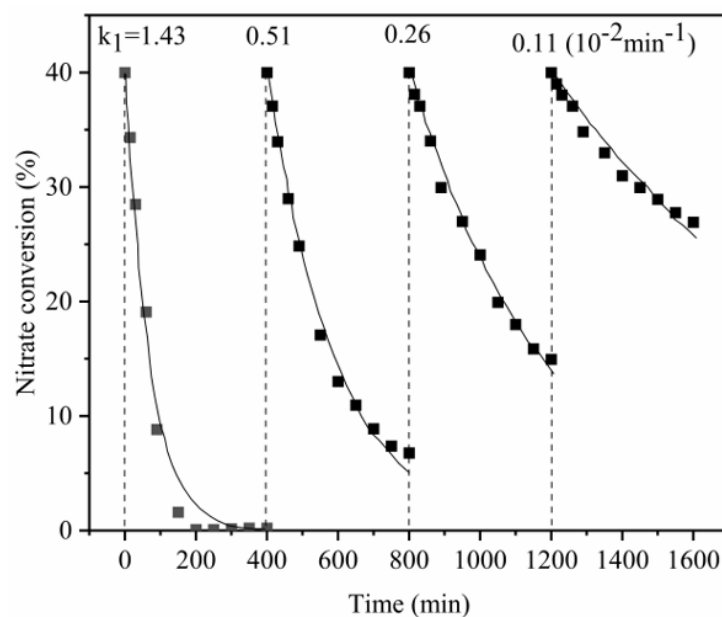


Figure 7. Repetitive reactions of 15 g/L alloy with nitrate; nitrate solution was repeatedly recharged to 40 mg/L every 400 min. (The scatter point was the measured value, and the line was the fitting curve).

4. Conclusions

This study induced the Al-Fe alloy in nitrate removal. Water activation pre-treatment substantially promoted the breakage of the surface passive oxide film, resulting in a higher ultimate nitrate removal (98%) than that when copper deposited alloy (66%) and acid/alkali/Cl⁻ activated alloy (no enhancement) were used.

Al-Fe30 displayed the highest activity for NO₃⁻ conversion and the highest Al₁₃Fe₄ content (XRD results) and was selected for nitrate reduction. Ninety-eight percent removal efficiency and 19% N₂ selectivity were obtained under the optimum operational conditions of 15 g/L Al-Fe30, 150 min reaction time and without pH adjustment. The repetition of the nitrate reduction by Al-Fe30 was performed, and the reduction was repeated for four times until the reduction level was significantly reduced. The nitrate removal process was successfully elucidated using several first-order reaction models.

Compared with the previous paper using Al-Fe alloy for nitrate reduction [10], the N₂ selective production showed limited advantages. The Al₁₃Fe₄ fraction in the alloy synthesized in these studies were all limited (XRD results). The similar low N₂ selective in these studies could be expected. Another synthesis method is now under development in the author's lab, which is aimed at the improvement of intermetallic component content in the Al-Fe alloy and the possible N₂ selective production improvement. Besides, multiple factor conditions, alloy powder and nitrate reduction using other reductant was affected by temperature and initial pH value and will be further studied in the lab. In addition, researchers will conduct real wastewater treatment experiments based on the parameter optimization results of this article.

Supplementary Materials: The following supporting information can be downloaded at: <https://www.mdpi.com/article/10.3390/w15173122/s1>, Figure S1: Variations of pH with respect to time; Figure S2: XRD patterns of different Al-Fe alloys; Table S1: Correlation coefficient based on different reaction orders.

Author Contributions: Methodology, X.M.; Supervision, Z.L., L.Z. (Lingling Zhang), S.C. and X.W.; Writing—original draft, L.Z. (Lei Zheng). All authors have read and agreed to the published version of the manuscript.

Funding: This work was supported by a joint program in cooperation with the National Taipei University of Technology (Grant Agreement No. TW201603).

Data Availability Statement: Data cannot be disclosed due to internal requirements. If you would like data, please contact the corresponding author (Zheng, L.) by email.

Acknowledgments: This research was supported by a joint program in cooperation with the National Taipei University of Technology (Grant Agreement No. TW201603). The authors gratefully acknowledge this support.

Conflicts of Interest: The authors declare no conflict of interest.

References

1. Yun, Y.; Li, Z.; Chen, Y.-H.; Saino, M.; Cheng, S.; Zheng, L. Reduction of Nitrate in Secondary Effluent of Wastewater Treatment Plants by Fe-0 Reductant and Pd-Cu/Graphene Catalyst. *Water Air Soil Pollut.* **2016**, *227*, 111. [CrossRef]
2. Wang, Y.; Zhao, H.; Zhao, G. Iron-copper bimetallic nanoparticles embedded within ordered mesoporous carbon as effective and stable heterogeneous Fenton catalyst for the degradation of organic contaminants. *Appl. Catal. B Environ.* **2015**, *164*, 396–406. [CrossRef]
3. Suzuki, T.; Moribe, M.; Oyama, Y.; Niinae, M. Mechanism of nitrate reduction by zero-valent iron: Equilibrium and kinetics studies. *Chem. Eng. J.* **2012**, *183*, 271–277. [CrossRef]
4. Barrabes, N.; Sa, J. Catalytic nitrate removal from water, past, present and future perspectives. *Appl. Catal. B Environ.* **2011**, *104*, 1–5. [CrossRef]
5. Kim, M.-S.; Chung, S.-H.; Yoo, C.-J.; Lee, M.S.; Cho, I.-H.; Lee, D.-W.; Lee, K.-Y. Catalytic reduction of nitrate in water over Pd-Cu/TiO₂ catalyst: Effect of the strong metal-support interaction (SMSI) on the catalytic activity. *Appl. Catal. B Environ.* **2013**, *142*, 354–361. [CrossRef]
6. Yun, Y.; Li, Z.; Chen, Y.H.; Saino, M.; Cheng, S.; Zheng, L. Catalytic reduction of nitrate in secondary effluent of wastewater treatment plants by Fe-0 and Pd-Cu/gamma-Al₂O₃. *Water Sci. Technol.* **2016**, *73*, 2697–2703. [CrossRef] [PubMed]

7. Armbruester, M.; Kovnir, K.; Friedrich, M.; Teschner, D.; Wowsnick, G.; Hahne, M.; Gille, P.; Szentmiklosi, L.; Feuerbacher, M.; Heggen, M.; et al. $\text{Al}_{13}\text{Fe}_4$ as a low-cost alternative for palladium in heterogeneous hydrogenation. *Nat. Mater.* **2012**, *11*, 690–693. [[CrossRef](#)] [[PubMed](#)]
8. Piccolo, L.; Kibis, L. The partial hydrogenation of butadiene over $\text{Al}_{13}\text{Fe}_4$: A surface-science study of reaction and deactivation mechanisms. *J. Catal.* **2015**, *332*, 112–118. [[CrossRef](#)]
9. Lee, J.M.; Kang, S.B.; Sato, T.; Tezuka, H.; Kamio, A. Evolution of iron aluminide in Al/Fe in situ composites fabricated by plasma synthesis method. *Mater. Sci. Eng. A Struct. Mater. Prop. Microstruct. Process.* **2003**, *362*, 257–263. [[CrossRef](#)]
10. Xu, J.; Pu, Y.; Qi, W.-K.; Yang, X.J.; Tang, Y.; Wan, P.; Fisher, A. Chemical removal of nitrate from water by aluminum-iron alloys. *Chemosphere* **2017**, *166*, 197–202. [[CrossRef](#)]
11. Bao, Z.; Hu, Q.; Qi, W.; Tang, Y.; Wang, W.; Wan, P.; Chao, J.; Yang, X.J. Nitrate reduction in water by aluminum alloys particles. *J. Environ. Manag.* **2017**, *196*, 666–673. [[CrossRef](#)] [[PubMed](#)]
12. Deng, Z.-Y.; Ferreira, J.M.F.; Tanaka, Y.; Ye, J. Physicochemical mechanism for the continuous reaction of $\text{-Al}_2\text{O}_3$ -modified aluminum powder with water. *J. Am. Ceram. Soc.* **2007**, *90*, 1521–1526. [[CrossRef](#)]
13. Liou, Y.H.; Lo, S.L.; Lin, C.J.; Hu, C.Y.; Kuan, W.H.; Weng, S.C. Methods for accelerating nitrate reduction using zerovalent iron at near-neutral pH: Effects of H-2-reducing pretreatment and copper deposition. *Environ. Sci. Technol.* **2005**, *39*, 9643–9648. [[CrossRef](#)] [[PubMed](#)]
14. Ho, C.-Y. Hydrolytic reaction of waste aluminum foils for high efficiency of hydrogen generation. *Int. J. Hydrogen Energy* **2017**, *42*, 19622–19628. [[CrossRef](#)]
15. Soltis, J. Passivity breakdown, pit initiation and propagation of pits in metallic materials-Review. *Corros. Sci.* **2015**, *90*, 5–22.
16. McCafferty, E. Sequence of steps in the pitting of aluminum by chloride ions. *Corros. Sci.* **2003**, *45*, 1421–1438.
17. Murer, N.; Buchheit, R.G. Stochastic modeling of pitting corrosion in aluminum alloys. *Corros. Sci.* **2013**, *69*, 139–148. [[CrossRef](#)]
18. Khalil, A.M.E.; Eljamal, O.; Jribi, S.; Matsunaga, N. Promoting nitrate reduction kinetics by nanoscale zero valent iron in water via copper salt addition. *Chem. Eng. J.* **2016**, *287*, 367–380. [[CrossRef](#)]
19. Newell, A.; Thampi, K.R. Novel amorphous aluminum hydroxide catalysts for aluminum-water reactions to produce H-2 on demand. *Int. J. Hydrogen Energy* **2017**, *42*, 23446–23454. [[CrossRef](#)]
20. Gai, W.-Z.; Deng, Z.-Y. Effect of initial gas pressure on the reaction of Al with water. *Int. J. Hydrogen Energy* **2014**, *39*, 13491–13497. [[CrossRef](#)]
21. Bunker, B.C.; Nelson, G.C.; Zavadil, K.R.; Barbour, J.C.; Wall, F.D.; Sullivan, J.P.; Windisch, C.F.; Engelhardt, M.H.; Baer, D.R. Hydration of passive oxide films on aluminum. *J. Phys. Chem. B* **2002**, *106*, 4705–4713. [[CrossRef](#)]
22. Eom, K.S.; Kwon, J.Y.; Kim, M.J.; Kwon, H.S. Design of Al-Fe alloys for fast on-board hydrogen production from hydrolysis. *J. Mater. Chem.* **2011**, *21*, 13047–13051. [[CrossRef](#)]
23. Matilainen, A.; Pussi, K.; Diehl, R.D.; Hahne, M.; Gille, P.; Gaudry, E.; Loli, L.N.S.; McGuirk, G.M.; de Weerd, M.C.; Fournee, V.; et al. Structure of the monoclinic $\text{Al}_{13}\text{Fe}_4(010)$ complex metallic alloy surface determined by low-energy electron diffraction. *Phys. Rev. B* **2015**, *92*, 014109. [[CrossRef](#)]
24. Lubphoo, Y.; Chyan, J.-M.; Grisdanurak, N.; Liao, C.-H. Influence of Pd-Cu on nanoscale zero-valent iron supported for selective reduction of nitrate. *J. Taiwan Inst. Chem. Eng.* **2016**, *59*, 285–294. [[CrossRef](#)]
25. Liou, Y.H.; Lin, C.J.; Weng, S.C.; Ou, H.H.; Lo, S.L. Selective Decomposition of Aqueous Nitrate into Nitrogen Using Iron Deposited Bimetals. *Environ. Sci. Technol.* **2009**, *43*, 2482–2488. [[CrossRef](#)] [[PubMed](#)]
26. Su, C.M.; Puls, R.W. Nitrate reduction by zerovalent iron: Effects of formate, oxalate, citrate, chloride, sulfate, borate, and phosphate. *Environ. Sci. Technol.* **2004**, *38*, 2715–2720. [[CrossRef](#)]
27. Wada, K.; Hirata, T.; Hosokawa, S.; Iwamoto, S.; Inoue, M. Effect of supports on Pd-Cu bimetallic catalysts for nitrate and nitrite reduction in water. *Catal. Today* **2012**, *185*, 81–87. [[CrossRef](#)]

Disclaimer/Publisher’s Note: The statements, opinions and data contained in all publications are solely those of the individual author(s) and contributor(s) and not of MDPI and/or the editor(s). MDPI and/or the editor(s) disclaim responsibility for any injury to people or property resulting from any ideas, methods, instructions or products referred to in the content.